

Time-Domain Simulations of the Coupled Dynamics of Surface Riding Wave Energy Converter

Chungkuk Jin, Moo-Hyun Kim, HeonYong Kang

Abstract—A surface riding (SR) wave energy converter (WEC) is designed and its feasibility and performance are numerically simulated by the author-developed floater-mooring-magnet-electromagnetics fully-coupled dynamic analysis computer program. The biggest advantage of the SR-WEC is that the performance is equally effective even in low sea states and its structural robustness is greatly improved by simply riding along the wave surface compared to other existing WECs. By the numerical simulations and actuator testing, it is clearly demonstrated that the concept works and through the optimization process, its efficiency can be improved.

Keywords—Computer simulation, electromagnetics fully-coupled dynamics, floater-mooring-magnet, optimization, performance evaluation, surface riding, wave energy converter.

I. INTRODUCTION

As world population and environmental concern increase, so does the need for clean renewable energy. In particular, wave energy is considered to be a primary energy source from the ocean. It is clean, unlimited, and does not produce any waste. However, the wave-power output is highly variable depending on sea states and the survivability of the conversion system during storms is a big concern. In this regard, the SR WEC concept is devised by authors [1].

The SR-WEC utilizes direct-drive LEG (linear electric generator) and the slopes produced by waves. The magnet continues to slide inside coil while riding along the generated wave slopes. Throughout all levels of sea states, lower wave heights mean shorter wavelengths. Therefore, the wave slopes tend to remain minimally variable through all sea states when compared to other WEC's [2]-[5]. This means that the SR-WEC is equally efficient in low sea states, which is a major portion of the sea states of any given site. Therefore, it has greatly extended operating window compared to other existing WECs.

Second, SR-WEC is simply riding along the wave surface, so minimally resists against wave-induced dynamic force. Therefore, the structural robustness in high sea states (or storms) is greatly improved. Also, by operating on the free surface, the cost and effort related to the deployment, repair, and removal tend to be much less compared to other existing WECs.

In the present paper, computer-simulation numerical tools

are developed by authors to assess the fully-coupled dynamics among waves, floaters, sliding magnet, and electromagnetic field between magnet and coil.

II. NUMERICAL MODEL

A. Configuration

Fig. 1 shows the configuration of the SR-WEC. The device is made up of a sliding magnet and inner and outer cylinders. The major parameters of the SR-WEC are summarized in Table I. The magnet assembly, made of a neodymium (NdFeB) magnet with lamination steels, is located inside the inner cylinder. The armature assembly, comprised of a coil and lamination steels, is attached to the inside shell of the outer cylinder. The magnet assembly is only allowed to move along the fixed center axle. The spring/damper system at both ends mitigates collision-induced damage. A single point mooring (SPM) is to be designed for the minimum station-keeping purpose. The SPM is to be linked to the SR-WEC at the middle bottom location. The linear generator parameters, given in Table I, are obtained from a previous study [6].

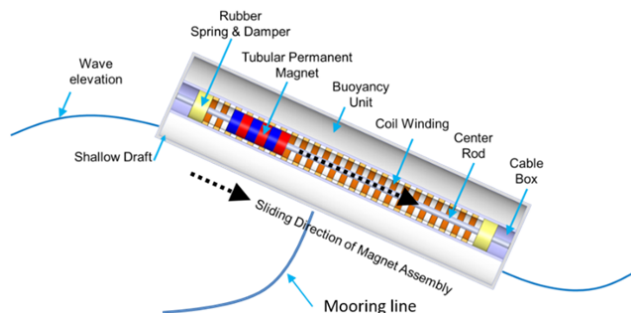


Fig. 1 Configuration of the SR-WEC

B. Working Principle

The outer cylinder, in general, has 6-degree-of-freedom (DOF) motions in waves. However, the elongated slender shape is to be aligned with the wave direction i.e. the outer cylinder tends to weathervane along the wave direction. Therefore, when riding along the wave surface, pitch motion is to be dominant. As the inclination angle θ_s of the SR-WEC is greater than the minimum sliding angle in the lubricated condition, the magnet assembly has the sliding force F_s in the sliding direction by gravity, which can be expressed as:

$$F_s = m_i g (\sin \theta_s - \mu_f \cos \theta_s) \quad (1)$$

Chungkuk Jin and Moo-Hyun Kim are with the Department of Ocean Engineering, Texas A&M University, College Station, TX, 77843 USA (e-mail: kenjin0519@gmail.com, m-kim3@tamu.edu)

HeonYong Kang is with the Department of Ocean Engineering, Texas A&M University, College Station, TX, 77843 USA (corresponding author, phone: 979-218-0846; e-mail: ga0prodg@tamu.edu).

where μ_f is the friction coefficient, and m_i is the mass of the magnet assembly.

TABLE I
MAJOR PARAMETERS OF THE SR-WEC

Component	Item	Value	Unit
Outer cylinder with armature assembly	Length	8.0	m
	Diameter	2.6	m
	Mass	21,365	kg
Inner cylinder with magnet assembly (NdFeB magnet with lamination steels)	Length	1.0	m
	Diameter	0.38	m
	Mass	403	kg
	Air gap	0.5	cm
Generator Parameters [10]	Phase resistance	4.58	Ω
	Phase inductance	190	mH
	Pole pitch	72	mm
	Coil pitch	72	mm
Mooring line (Studlink Chain)	Nominal diameter	1.5	cm
	Length	100	m
	Mass/unit length	4.9	kg/m

C. Numerical Model in Time-Domain

Time-domain analysis of the SR-WEC is completed by using the in-house program, CHARM3D, which can solve the coupled dynamics of the floater-mooring system. The 6 DOF equations of motion for the outer cylinder in time-domain are based on the Cummins equation. The added mass, the radiation damping, and hydrostatic restoring coefficients, and first-order wave forces and moments, which are required for time-domain analysis, are estimated in the frequency domain using a diffraction-radiation 3D panel program. Horizontal and vertical viscous drag forces are further added in the time-domain simulation using the modified Morison equation. The drag coefficient of 0.5 is used and the drag forces are applied at the center of gravity. The viscous damping moments are also applied for rotational moments, and a critical damping ratio of 0.03 is assumed in this study.

The dynamic model of the mooring line is based on rod theory [7], and the Galerkin finite element method is used for further implementation. The outer cylinder is connected to the mooring line by the hinged boundary condition. The detailed formulations of the program can be found in [8]-[10].

1 DOF equation of motion for the inner cylinder is defined with a coordinate along the center axle of the outer cylinder; thus, the relative displacement is calculated with respect to outer cylinder's center. Then, the additional force, i.e., inertia force in the sliding direction (mass of the inner cylinder multiplied by the acceleration of the outer cylinder) should also be considered. Also, when the normal contact force causing friction is calculated, the surge and heave accelerations of the cylinder need to be considered. Generally, their influences are expected to be much less compared to the gravity force.

The coupling of both cylinders is completed by introducing the magnetic force between the magnet and armature assemblies and adopting conservation of momentum to define the collision at both ends. The magnetic force calculation procedures are shown in Fig. 2. When the inner cylinder i.e. the magnet assembly does not hit the ends, the time integration with the consideration of the magnetic force solves the relative displacement and velocity of the inner magnet. However, as the inner cylinder is about to hit the end location, a combination of the conservation of momentum and the coefficient of restitution is applied at that moment. By assuming that the mass of the outer cylinder is much larger than that of the inner cylinder, the relative velocity after hitting the wall can approximately be obtained by the previous velocity of the magnet assembly times the coefficient of restitution in the negative direction. Authors conducted the validation of our linear-generator scheme by comparing the power output results with those of the experimental results by [6] under irregular waves. Also, the dynamics of the inner cylinder is also validated through our experiments with actuators to gain the minimum sliding angle (friction coefficient) and the coefficient of restitution.

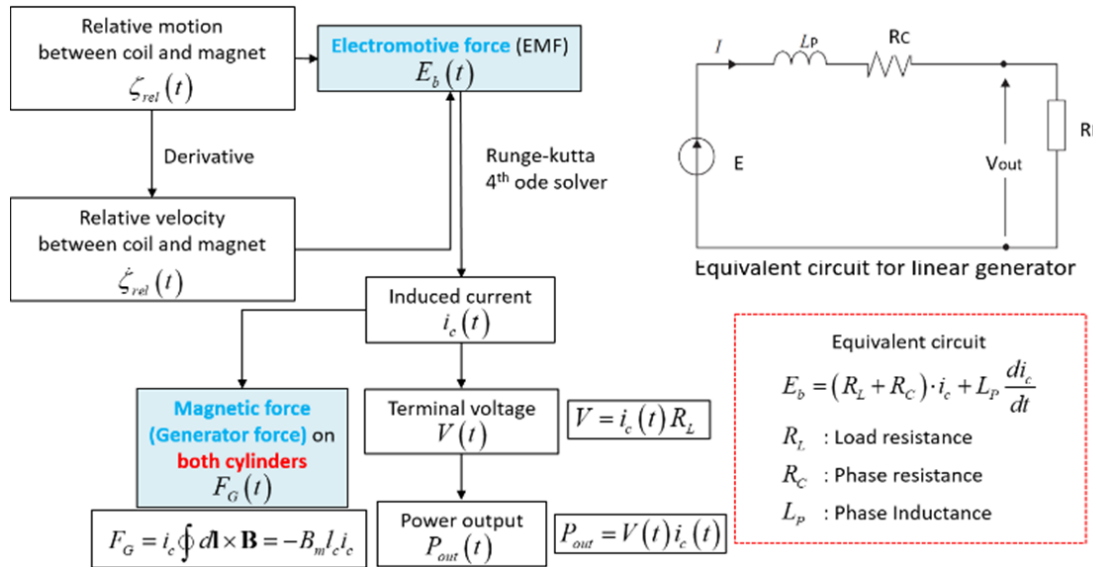


Fig. 2 Numerical scheme of magnetic force and power output

D.Environmental Condition

The time histories of wave elevation are generated by the superposition of numerous linear wave components from the JONSWAP wave spectrum. 100 linear wave components are superposed, and randomly perturbed intervals are used to prevent the signal repetition. While different significant wave heights (H_s) from 1.0 m to 3.5 m with various peak periods (T_p) from 5.0 sec to 11.0 sec are simulated, a typical case of $H_s=2$ m and $T_p=6$ sec is presented in the study. Simulation time for each case is 15 minutes, and the wave direction is parallel with the longitudinal direction of the SR-WEC, i.e., 0 degrees.

III. RESULTS AND DISCUSSIONS

A. Frequency-Domain Analysis

First, the pitch RAO (response amplitude operator) is calculated by using the 3D diffraction/radiation panel program. As expected, resonance can be seen at the pitch natural frequency = 1.65 rad/s. The convergence of the results is also tested with increasing the number of panel numbers, which shows good convergence. The hydrodynamic coefficients are subsequently used in the ensuing time-domain simulations.

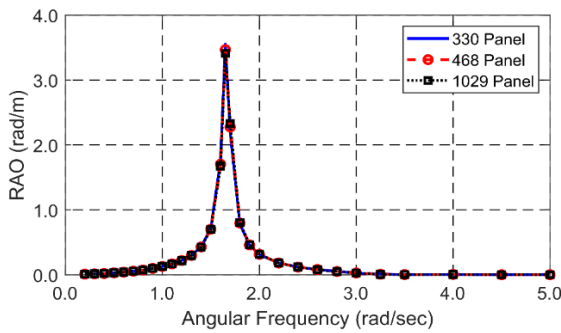


Fig. 3 Undamped pitch RAOs under different panel numbers

B. Time-Domain Analysis

In the time-domain simulation, the coupled dynamics and power outputs are calculated and several different parametric cases are compared i.e. effects of power take-off system, sliding length of the magnet assembly, and mass of the magnet assembly.

First, Figs. 4 and 5 show the effect of the power take-off (PTO) system on the sliding efficiency and generated power output. In general, magnetic forces are proportional to electric currents and the electric currents become smaller as resistances R increase. Therefore, as can be seen in Figs. 4 and 5, larger R results in larger magnet displacements and velocities. However, the generated power is proportional to the electric current, so smaller electric current results in smaller power output. Therefore, there should be an optimal combination of the linear generator parameters.

Fig. 6 shows the effect of the given magnet sliding length on the generated power outputs. We can see that the initially given total sliding length also influences the power output.

Finally, in Fig. 7 is the effect of magnet mass on the generated power output. In this case, it is clear that heavier

magnet mass results in larger power output. In all cases, the generated power is highly fluctuating, which is the typical feature in all WECs in random seas. The maximum power out in Fig. 7 is about 9 kW, which is relatively effective considering the size of WEC and the low sea state.

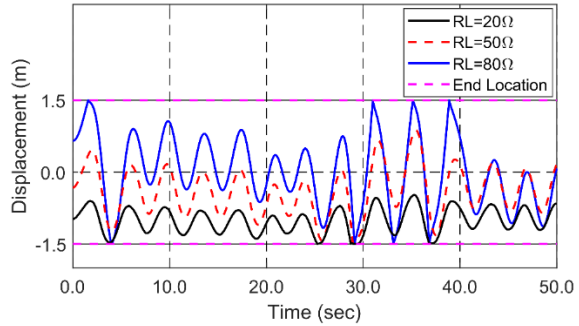


Fig. 4 Time histories of displacements of the magnet assembly at different load resistances ($H_s = 2.0$, $T_p = 6.0$, mass of the magnet assembly = 400 kg, sliding length = 3 m, RL = load resistance)

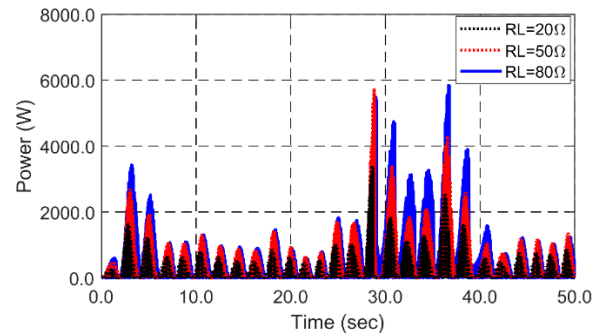


Fig. 5 Time histories of power outputs at different load resistances ($H_s = 2.0$, $T_p = 6.0$, mass of the magnet assembly = 400 kg, sliding length = 3 m, RL = load resistance)

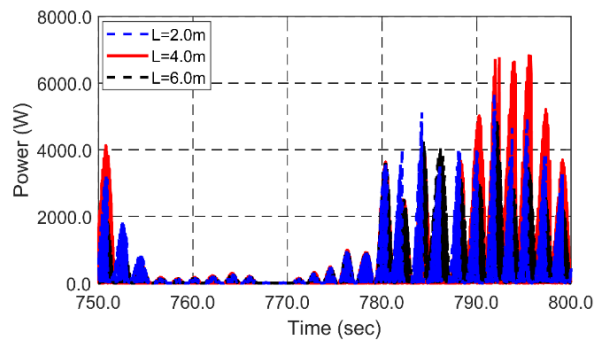


Fig. 6 Time histories of power outputs at different sliding lengths ($H_s = 2.0$, $T_p = 6.0$, mass of the magnet assembly = 400 kg, RL = 80 Ω)

IV. CONCLUSION

This study presents the feasibility of the developed SR WEC. A time-domain program was developed to solve the floater-mooring-generator fully-coupled dynamics. The computer simulation results were validated against the scaled testing with actuators. By the numerical simulations and actuator testing, it

was clearly demonstrated that the concept works and its performance depend on design parameters. Through the optimization process with varying design parameters, its efficiency can be improved. The maximum power out in the case studies was about 9 kW, which is relatively effective compared to other WECs considering the size of SR-WEC and the low sea state.

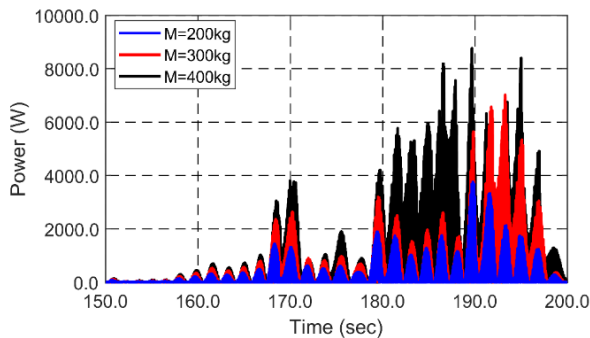


Fig. 7 Time histories of power outputs at different masses of the magnet assembly ($H_s = 2.0$, $T_p = 6.0$, sliding length = 4 m, RL = 80 Ω)

ACKNOWLEDGMENT

This research is financially supported by US DOE EERE WPTO project.

REFERENCES

- [1] H.Y. Kang and M.H. Kim, "Method and apparatus for wave energy conversion," US Patent 15896335, 2018.
- [2] I.-H. Cho, J. Kim, and M.-H. Kim, "Numerical calculation and experiment of a heaving-buoy wave energy converter with a latching control," *Ocean Systems Engineering*, vol. 9, pp. 1–19, March 2019.
- [3] W. Koo and M.-H. Kim, "A time-domain simulation of an oscillating water column with irregular waves," *Ocean Systems Engineering*, vol. 2, pp. 147–158, June 2012.
- [4] Y. Gao, S. Shao, H. Zou, M. Tang, H. Xu, and C. Tian, "A fully floating system for a wave energy converter with direct-driven linear generator," *Energy*, vol. 95, pp. 99–109, January 2016.
- [5] E. Lejerskog, C. Boström, L. Hai, R. Waters, and M. Leijon, "Experimental results on power absorption from a wave energy converter at the Lysekil wave energy research site," *Renewable Energy*, vol. 77, pp. 9–14, May 2015.
- [6] J. Prudell, M. Stoddard, E. Amon, T. K. A. Brekken, and A. von Jouanne, "A permanent-Magnet Tubular Linear Generator for Ocean Wave Energy Conversion," *IEEE Transactions on Industry Application*, vol. 46, pp. 2392–2400, November/December 2010.
- [7] D. L. Garrett, "Dynamic analysis of slender rods," *Journal of Energy Resources Technology*, vol. 104 pp. 302–306, December 1982.
- [8] Z. Ran, M. H. Kim, and W. Zheng, "Coupled dynamic analysis of a moored spar in random waves and currents (time-domain versus frequency-domain analysis)," *Journal of Offshore Mechanics and Arctic Engineering*, vol. 121, pp. 194–200, August 1999.
- [9] B. J. Koo and M. H. Kim, "Hydrodynamic interactions and relative motions of two floating platforms with mooring lines in side-by-side offloading operation," *Applied Ocean Research*, vol. 27, pp. 292–310, December 2005.
- [10] C. Jin and M.-H. Kim, "Time-domain hydro-elastic analysis of a SFT (submerged floating tunnel) with mooring lines under extreme wave and seismic excitations," *Applied Sciences*, vol. 8, pp. 2236, November 2018.